Time-Resolved Fourier Transform Infrared Spectroscopy of the Polarizable Proton Continua and the Proton Pump Mechanism of Bacteriorhodopsin

Jianping Wang and Mostafa A. El-Sayed
Laser Dynamics Laboratory, School of Chemistry and Biochemistry, Georgia Institute of Technology, Atlanta, Georgia 30332 USA

ABSTRACT Nanosecond-to-microsecond time-resolved Fourier transform infrared (FTIR) spectroscopy in the 3000–1000-cm^{-1} region has been used to examine the polarizable proton continua observed in bacteriorhodopsin (bR) during its photocycle. The difference in the transient FTIR spectra in the time domain between 20 ns and 1 ms shows a broad absorption continuum band in the 2100–1800-cm^{-1} region, a bleach continuum band in the 2500–2150-cm^{-1} region, and a bleach continuum band above 2700 cm^{-1}. According to Zundel (G. Zundel, 1994, *J. Mol. Struct.* 322:33–42), these continua appear in systems capable of forming polarizable hydrogen bonds. The formation of a bleach continuum suggests the presence of a polarizable proton in the ground state that changes during the photocycle. The appearance of a transient absorption continuum suggests a change in the polarizable proton or the appearance of new ones. It is found that each continuum has a rise time of less than 80 ns and a decay time component of ~300 μs. In addition, it is found that the absorption continuum in the 2100–1800-cm^{-1} region has a slow rise component of 190 ns and a fast decay component of ~60 μs. Using these results and those of the recent x-ray structural studies of bR_{570} and M_{412} (H. Luecke, B. Schobert, H.T. Richter, J.-P. Cartailler, and J. K. Lanyi, 1999, *Science* 286:255–260), together with the already known spectroscopic properties of the different intermediates in the photocycle, the possible origins of the polarizable protons giving rise to these continua during the bR photocycle are proposed. Models of the proton pump are discussed in terms of the changes in these polarizable protons and the hydrogen-bonded chains and in terms of previously known results such as the simultaneous deprotonation of the protonated Schiff base (PSB) and Tyr185 and the disappearance of water molecules in the proton release channel during the proton pump process.

INTRODUCTION

Bacteriorhodopsin (bR), present in the purple membrane of *Halobacterium salinarium*, functions as a proton pump upon visible light absorption (Stoeckenius and Lozier, 1974; Birge, 1981; Mathies et al., 1991; Rothschild, 1992; El-Sayed, 1992; Ebrey, 1993; Lanyi, 1993). There are 248 amino acid residues in the single polypeptide chain, arranged in seven α-helices (Henderson, 1979). The three-dimensional structure of bR has been determined at high resolution by a number of researchers, using cryoelectron microscopy (Henderson et al., 1990) and x-ray crystallography (Pebay-Peyroula et al., 1997; Luecke et al., 1998; Essen et al., 1998). The retinal chromophore that is covalently bound to Lys216 through a protonated Schiff base (PSB) undergoes a photoisomerization from all-*trans* to 13-*cis* and triggers a cyclic thermal reaction that involves a series of photointermediates, J, K, L, M_1, M_2, N, and O, with lifetimes ranging from half a picosecond to tens of milliseconds:

$$bR \xrightarrow{h\nu} bR^* \xrightarrow{500\ fs} J \xrightarrow{2\ ps} K \xrightarrow{1\ \mu s} L \xrightarrow[-H^+]{60\ \mu s}$$

$$M_1 \leftrightarrow M_2 \xrightarrow[+H^+]{ms} N \rightarrow O \rightarrow bR$$

The nature of J is under discussion, and recent results suggest it is an excited-state conformer of all-*trans* retinal (Atkinson et al., 2000). Retinal, protein residue, and hydrogen bonding structural changes are expected to be associated with the bR photocycle. Upon retinal *cis-trans* photoisomerization and K formation, there are changes in the protein peptide backbone vibration frequency (Earnest et al., 1986), in the hydrogen-bonded network near the retinal (Kandori et al., 1998), as well as in the O-H stretching vibration of a water molecule as shown by using trapping technique and difference Fourier transform infrared (FTIR) spectroscopy at near 80 K (Maeda et al., 1992; Fischer et al., 1994). Upon M formation, the difference FTIR spectrum in the amide I and amide II bands suggest large changes in the protein secondary structure involving one or more helices (Rothschild, 1992). Room-temperature, time-resolved FTIR reveals protein structural changes that are partially blocked at low temperature, such as a greater degree of deprotonation of Asp96 in the L intermediate (Chen and Braiman, 1991). Large changes in the secondary and tertiary structures of bR upon N formation have been reported by using

Received for publication 14 August 2000 and in final form 2 November 2000.

Address reprint requests to Dr. Mostafa A. El-Sayed, Laser Dynamics Laboratory, School of Chemistry and Biochemistry, Georgia Institute of Technology, Atlanta, GA 30332-0400. Tel.: 404-894-0292; Fax: 404-894-0294; E-mail: Mostafa.El-Sayed@chemistry.gatech.edu.

0006-3495/01/02/961/11 $2.00

neutron and x-ray diffraction techniques (Dencher et al., 1990; Papadopoulos et al., 1990; Koch et al., 1991; Oka et al., 1999) and by using FTIR difference spectroscopy (Rothschild et al., 1990b; Nilsson et al., 1995). In the L-M transition, it is now established that a proton is transferred from the PSB to Asp85 (Braiman et al., 1988) and another proton appears on the extracellular surface (Heberle and Dencher, 1992; Alexiev et al., 1995). The origin of the latter (and thus the mechanism of the proton pump) has been the subject of intense research recently and has been proposed to be or involve several groups, such as Arg82 (Otto et al., 1990; Balashov et al., 1993, 1995; Govindjee et al., 1996), Glu194 (Dioumaev et al., 1998), or Glu204 (Misra et al., 1997; Kandori et al., 1997; Richter et al., 1996; Brown et al., 1995, 1996). Recently, it has been proposed to be due to the polarizable hydrogen-bonded proton with the spectroscopic signature in the region of 1900–1800 cm^{-1} (Rammelsberg et al., 1998; Wang and El-Sayed, 2000). Earlier, an ionized water molecule within the active site was also proposed to be the source of this proton (El-Sayed et al., 1995). Very recently, the x-ray structural changes upon the formation of M in a D96N mutant has recently been reported (Luecke et al., 1999a), and a proposed proton pump mechanism has been suggested, which contradicts the FTIR results (Rammelsberg et al., 1998; Zscherp et al., 1999).

Thus, despite the great amount of structural information about bR and its deprotonated form, the molecular origin of the proton pumped to the surface and the details of the proton pump mechanism itself remains very much unsolved. It is hoped that with more time-resolved spectral studies together with theoretical calculations and the determination of the x-ray structure of the other intermediates, a final accurate picture of the proton pump process can be determined. The present work is an effort in this direction and is aimed at a detailed study of the time-resolved infrared continua spectra believed to be due to the changes in the polarizable hydrogen-bonded protons in bR and its intermediates.

By using model compounds, it has been suggested (Merz and Zundel, 1986) that the hydrogen bonds between a Schiff base and a carboxylic acid may show large proton polarizability and, therefore, give rise to several very broad absorption continua in the infrared frequency region of 2800–800 cm^{-1} (Zundel and Merz, 1984; Mueller et al., 1991; Olejnik et al., 1992). The difference infrared continua observed for low-temperature trapped intermediates between bR and M have been reported and discussed previously (Olejnik et al., 1992; Zundel, 1994). The assignment of the transient continuum observed in the region of 1900–1800 cm^{-1} to the polarizable proton being pumped to the extracellular surface has been suggested recently by time-resolved FTIR studies (Riesle et al., 1996; Rammelsberg et al., 1998), and was more recently supported by the correspondence between the kinetics of the continuum and that of M formation, as well as the isotope effect on the transient continuum spectrum (Wang and El-Sayed, 2000).

In the present study, we examine the time-resolved infrared continuum spectra in the 3000–1800-cm^{-1} region for different intermediates formed during the bR photocycle at physiological temperature in the tens of nanoseconds to the hundreds of microseconds time domain. The results suggest that the ground state of native bR has a polarizable hydrogen-bonded network that changes its nature upon the formation of K, leading to an observed time-dependent bleach continua in the 2500–2150-cm^{-1} region and above 2700 cm^{-1}. As a result, a new transient absorption continuum appears in the 2100–1800-cm^{-1} region. This transient absorption continuum band decays during the M formation (in ~60 μs), whereas the ground-state polarizable hydrogen bond recovers on a longer time scale (~300 μs). The observed results, combined with previously published optical and FTIR spectroscopic observations as well as the results of the recent x-ray studies are all used to discuss the nature of these polarizable proton bands and the possible proton pump mechanisms in bR.

MATERIALS AND METHODS Sample

Purple membrane was isolated from the *Halobacterium salinarium* strain ET1001 according to a general procedure (Stoeckenius and Lozier, 1974). Purple membrane fragments containing bR molecules are suspended in H_2O at pH 7. Concentrated bR samples are squeezed in between two CaF_2 plates to give an optical density at protein amide I and II bands (1700–1500 cm^{-1}) of ~0.5–1.0.

Time-resolved FTIR spectroscopy

The step-scan FTIR measurements were carried out on the Nicolet Magna-IR 860 spectrometer. A 50-MHz mercury-cadmium-telluride (MCT) detector (Kolmar Technologies, Inc., Congers, GA) was used, with appropriate ac- and dc-coupled preamplifiers that give a linear response with respect to the infrared light intensity. Data were taken with a temporal resolution of 20 ns, 100 ns, and 10 μs at a spectral resolution of 4 cm^{-1}. The spectral region covers 3000–800 cm^{-1} (a combination of the MCT detector cutoff at 800 cm^{-1} and the bandpass germanium filter cutoff at 3000 cm^{-1}) in the time domain of 20 ns to 1 ms. Transient signals were co-added five to six times to improve the signal-to-noise ratio. The pulsed excitation source is the output at 532 nm from a Nd:YAG laser (Quantum-Ray DCR-3, Mountain View, CA), with laser energy of 3 mJ/pulse at a repetition rate of ~4 Hz, which is triggered externally through the Nicolet Omnic software. All the measurements were carried out at room temperature.

RESULTS

Fig. 1 shows the time-resolved FTIR difference spectrum between the photointermediate spectrum formed at a delay time of 600 ns after laser excitation and that of bR ground state, in the 3000–1000-cm^{-1} frequency range. In the time-resolved difference spectra, the positive bands originate from the formation of photointermediates and the negative bands result from the ground-state depletion as bR mole-

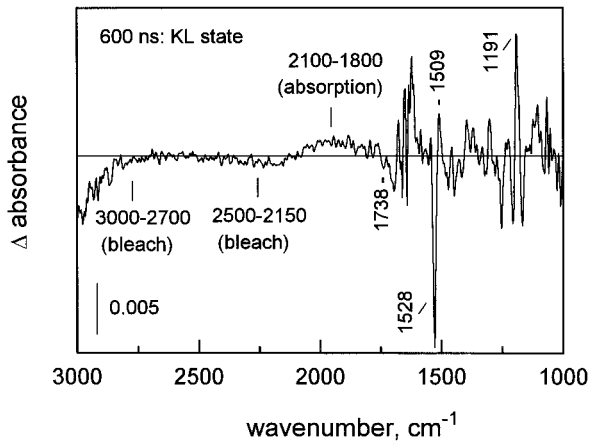

FIGURE 1 Time-resolved FTIR difference spectrum for bR in H_2O in the frequency range of 3000–1000 cm^{-1}, measured at room temperature. The spectrum is taken at a delay time of 600 ns, showing the difference between the spectrum of bR and KL state. Continuum band features are observed in the frequency regions of 3000–2700 cm^{-1} as a bleach, 2500–2150 cm^{-1} as a bleach, and 2100–1800 cm^{-1} as a transient absorption.

cules absorb light and go through the photocycle. The spectrum at the 600-ns delay corresponds to the transition stage from bR to the K (or KL) intermediate. The sharp band positions and relative intensities of the bands in this spectrum, such as 1528, 1509, and 1191 cm^{-1}, are found to be in good agreement with the 600–800-ns averaged spectrum in previous published reports (Sasaki et al., 1993; Wolfgang et al., 1996). The noise in the 1700–1540-cm^{-1} region is due to the overlap with the intense water-bending vibration absorption.

Three broad continua are shown in the 3000–1800-cm^{-1} frequency region. Two bleach continua are observed, one in the 2500–2150-cm^{-1} region and the other one in the 3000–2700-cm^{-1} region. One transient absorption continuum band is observed in the 2100–1800-cm^{-1} region. In the spectral region of 2800–2200 cm^{-1}, a weak and broad continuum band has been observed previously (Olejnik et al., 1992) in the trapped K and L minus bR difference spectra obtained at low temperature. These authors attributed such a broad band to the formation of at least one hydrogen bond in which the proton is not well localized. A recent report (Kandori et al., 1998), however, showed only a broad continuum bleach band in the 3000–2700-cm^{-1} region in the K minus bR difference spectrum obtained at 77 K, but not in the 2800–2200-cm^{-1} region. Our results show that both absorption and bleach bands in this frequency region can be observed at room temperature by using time-resolved step-scan FTIR. In addition, it should be noted that a continuum absorption band is shown in the 2100–1800-cm^{-1} region. In a recent report (Wolfgang et al., 1996), a continuum absorption band feature in the 1850–1800-cm^{-1} has also been observed in their 20–940-ns spectra. However, no nanosecond or microsecond transient spectra in the frequency region above 2000 cm^{-1} have ever been reported so far.

Fig. 2 shows the observed spectra in the 3000–1000-cm^{-1} region that are taken at selected delay times (from 50 ns to 950 μs) after bR has been photolyzed with 8-ns laser pulses at 532 nm. It should be noted that in both Figs. 1 and 2, the spectral sensitivity has been increased to observe the weak continuum. As a result, the strong bands at 1528 cm^{-1} and 1191 cm^{-1} are off scale. It is found that the transient absorption in the 2100–1800-cm^{-1} region is observed at 50 ns (Fig. 2 *a*) as well as 10 μs (Fig. 2 *c*). At this time, the positive band at 1763 cm^{-1} (resulting from the C═O stretching mode of the protonated proton acceptor Asp85) appears, whereas the positive band at 1191 cm^{-1} showed a significant decrease in intensity relative to that in the 50-ns spectrum.

Fig. 3 compares the time dependence of the transient continua at 2100–1800 cm^{-1}, 2500–2150 cm^{-1}, and 3000–2700 cm^{-1} in the 20-ns to 1-μs time domain, with that of

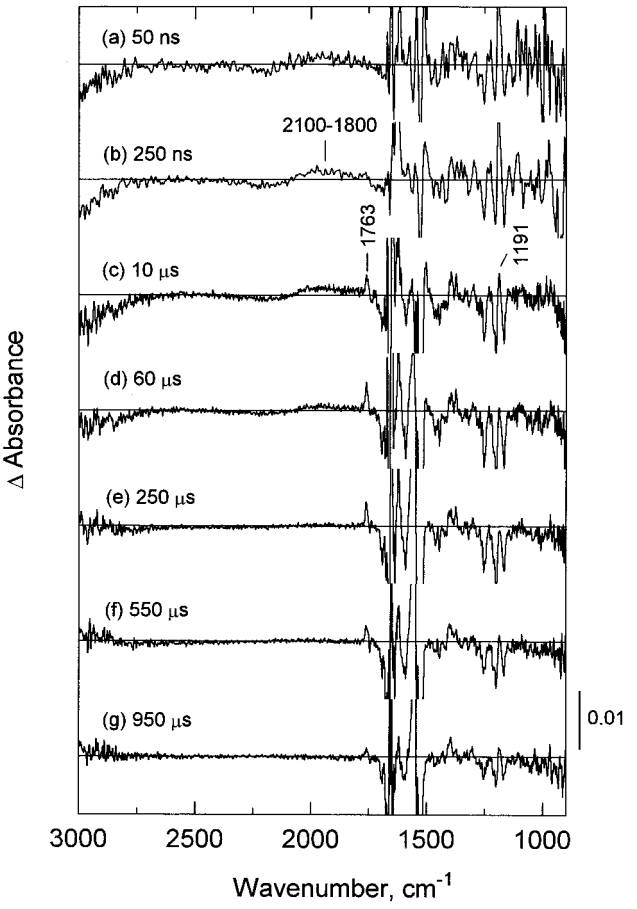

FIGURE 2 Time-resolved FTIR difference spectra for bR in H_2O in the frequency range of 3000–1000 cm^{-1}, measured at room temperature, and at various delay times as indicated: (*a*) 50 ns; (*b*) 250 ns; (*c*) 10 μs; (*d*) 60 μs; (*e*) 250 μs; (*f*) 550 μs; (*g*) 950 μs. This covers the time domain of the KL-L-M portion of the bR photocycle.

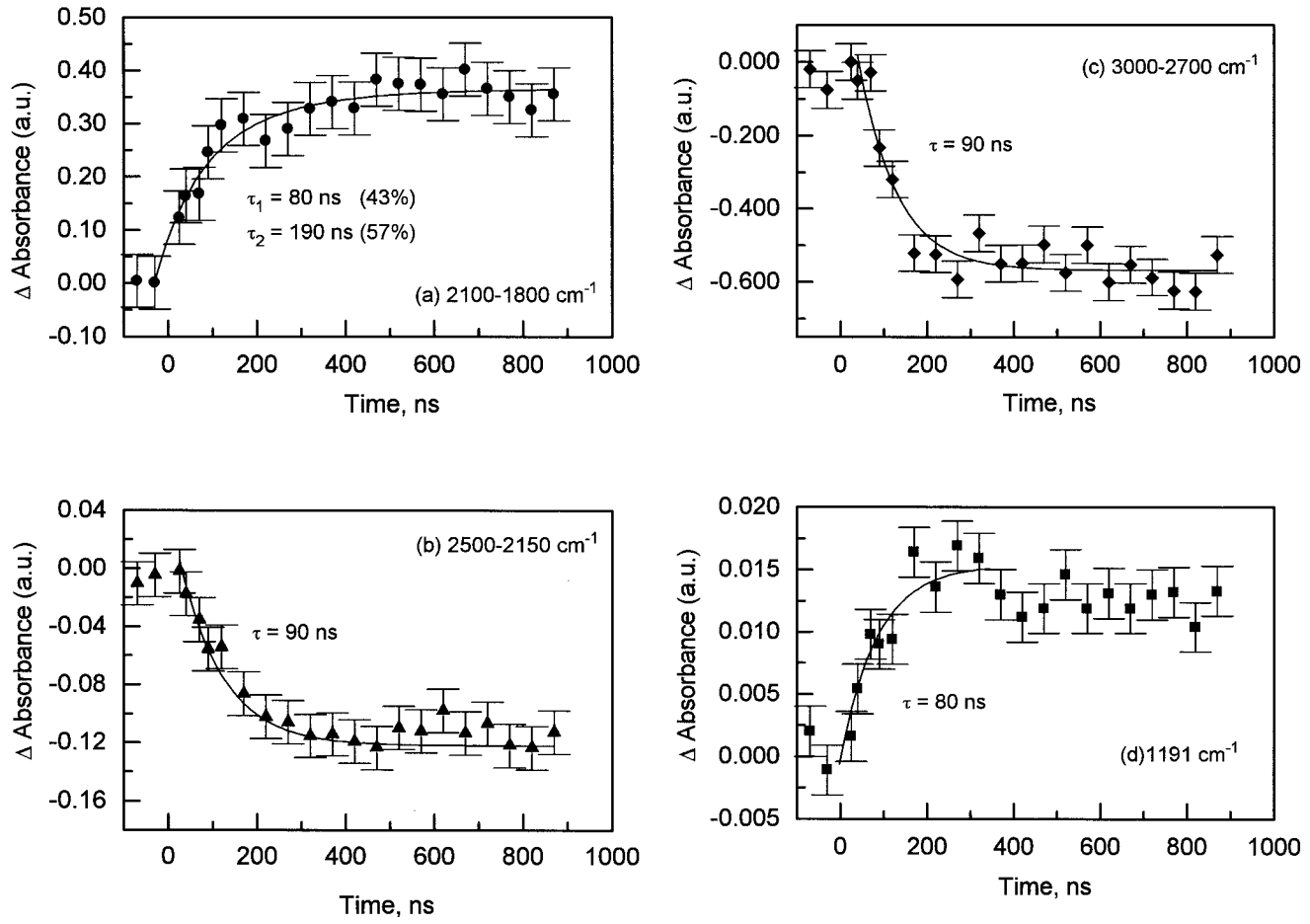

FIGURE 3 The initial temporal behavior of selected bands in the time domain of 20 ns to 1 μs. (*a*) The absorption continuum band in the 2100–1800-cm^{-1} region; (*b*) The bleach continuum 2500–2150-cm^{-1} region; (*c*) The bleach continuum 3000–2700-cm^{-1} region; (*d*) The retinal C—C stretching band at 1191 cm^{-1}. The fitted results are also shown, with the corresponding rise times given as: <80 ns; 190 ns for formation of the 2100–1800-cm^{-1} continuum absorption band; <90 ns for formation of the 2500–2150-cm^{-1} continuum bleach band; and <80 ns for the formation of the 1191-cm^{-1} band. The 80–90-ns short components observed correspond to the rise time of the detector suggesting that the initial component of these changes corresponds to the formation of the K intermediate.

the sharp positive band at 1191 cm^{-1} that is due to the 13-*cis* retinal C—C stretching in the K intermediate (Smith et al., 1986). Fitting the results gives two exponential rise components for the absorption continuum band at 2100–1800 cm^{-1}, with apparent rise times of <80 ns and 190 ns, respectively. The fast component is on the same time scale as that of the formation of the bleach bands (<90 ns; Fig. 3, *b* and *c*) and that of the 1191-cm^{-1} band (<90 ns; Fig. 3 *d*). It is known that the photoisomerization of retinal occurs in less than half a picosecond (Nuss et al., 1985; Petrich et al., 1987; Mathies et al., 1988; Van den Berg et al., 1990). Because the fingerprint band at 1191 cm^{-1} is associated with the K formation (Smith et al., 1986), its rise time should be ~3 ps instead of ~90 ns that we observed here. In fact, the 50–90-ns rise-time component appearing in all these spectra is determined by the rise time of the MCT detector used in the step-scan FTIR spectrometer. Our data thus indicate that the formation of the continuum bands is possibly associated with the retinal photoisomerization and the K formation. From Figs. 2 and 3, it is shown that the intensity of the observed continua is still developing in the time domain between 100 ns and a few microseconds (within which L is being formed), whereas the intensity of the retinal configuration sensitive band at 1191 cm^{-1} begins to decay within hundreds of nanoseconds (within which KL begins to decay (Wolfgang et al., 1996)), suggesting that these continua cannot be assigned to retinal vibrations.

Fig. 4 compares the decay of the absorption continuum band in the 2100–1800-cm^{-1} region (Fig. 4 *a*), the bleach continuum in the 2500–2150-cm^{-1} region (Fig. 4 *b*), the bleach continuum in the 3000–2700-cm^{-1} region (Fig. 4 *c*), and the transient absorption of the carbonyl band at 1763 cm^{-1} (Fig. 4 *d*) (which reflects the protonation of Asp85). The results show that the absorption continuum band in the 2100–1800-cm^{-1} region has two decay components, with lifetimes of ~60 and 300 μs. The fast component is similar

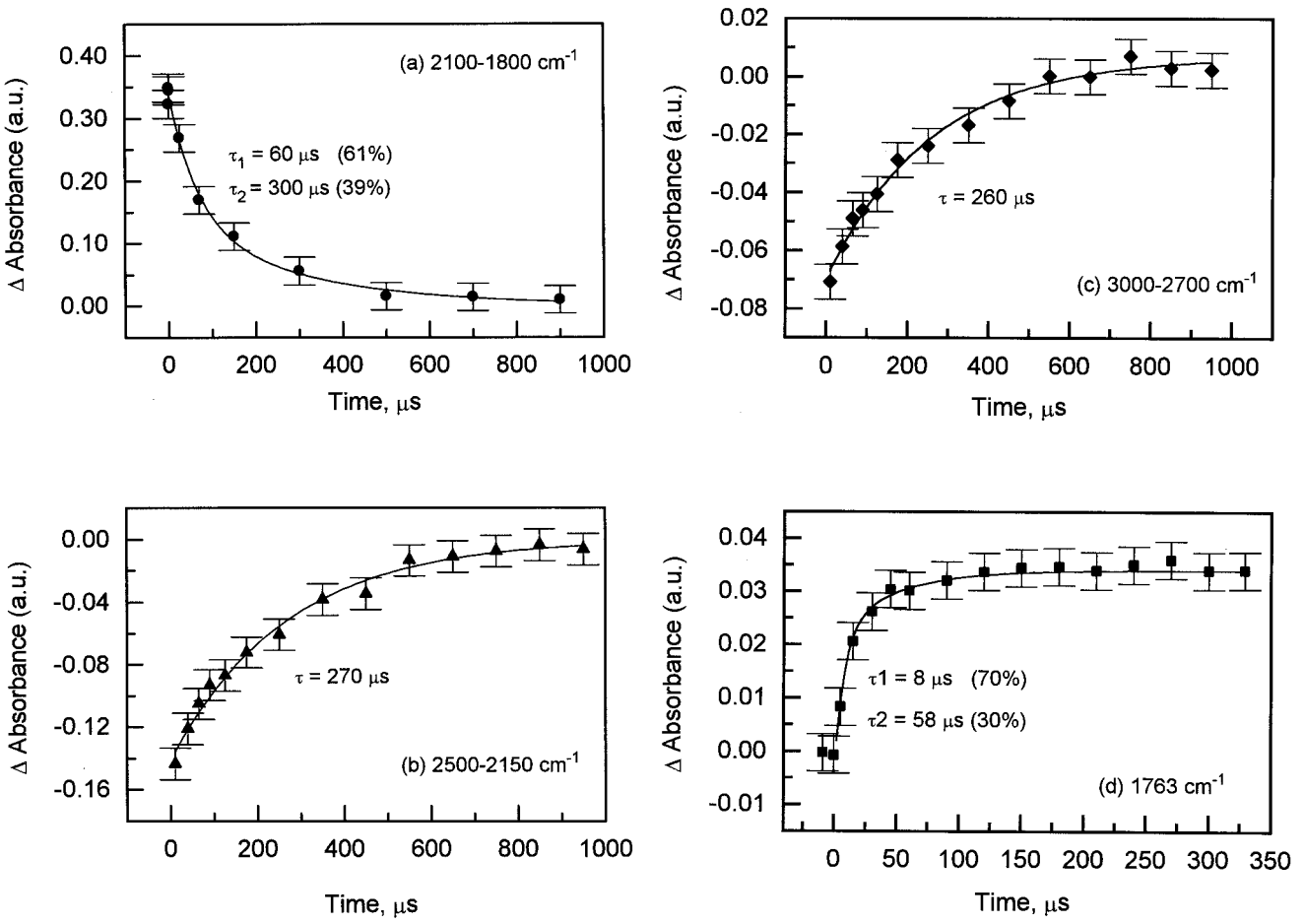

FIGURE 4 The long-time temporal behavior of selected bands in the time domain of micro- to milliseconds. (*a*) The decay of the transient absorption continuum band in the region of 2100–1800 cm^{-1}; (*b*) The recovery of the bleach continuum band in the region of 2500–2150 cm^{-1}; (*c*) The recovery of the bleach continuum band in the region of 3000–2700 cm^{-1}; (*d*) The rise of the C═O stretching mode absorption of Asp85 at 1763 cm^{-1}, an indicator of the protonation of Asp85. The fit to the observed results are also shown, with lifetimes given below: 60 μs and 300 μs for the decay of the 2100–1800-cm^{-1} band; 260–270 μs for the bleach recovery of the BC bands. The formation of the 1763-cm^{-1} band has two time constants of ~10 μs and ~60 μs, as also reported previously (Wang and El-Sayed, 2000).

to the slow rise-time component of the 1763-cm^{-1} band, (i.e., of the protonation of the proton acceptor, Asp85), which is found to be ~60 μs, as also seen in previous reports (Siebert et al., 1982; Wang and El-Sayed, 2000). On the other hand, the decay of the two bleach continua has a lifetime of ~260 μs, which is similar to the decay process of the long-lived component of the transient absorption continuum in the 2100–1800-cm^{-1} region (~300 μs), suggesting that these two continua belong to the same polarizable proton chain, or to two polarizable proton systems that are strongly coupled.

Deuterium effects on the observed broad continua band intensity have also been investigated in the present study. Fig. 5 shows a series of transient spectra of bR in D_2O solvent, at delay times of 200 ns, 600 ns, and 10 μs, respectively. It is obvious that there is no significant continuum absorption or bleach in D_2O observed in these regions as observed in H_2O (above 2700 cm^{-1} and in the regions of 2500–2150 cm^{-1} and 2100–1800 cm^{-1}). The distorted baseline and spectral noise in the 2750–2000-cm^{-1} spectral region are due to the strong absorption of the D—O stretching vibration mode of D_2O. This absorption could obscure the much weaker continua due to the polarizable deuterons. These results indicate that the observed continua in the bR/H_2O system show a deuterium isotopic effect and, therefore, involve proton oscillation. The deuterium isotopic effect has been previously reported in the 2100–1800-cm^{-1} region (Wang and El-Sayed, 2000).

DISCUSSION

The polarizable hydrogen-bonded continua

In a series of experiments and theoretical calculations, Zundel and co-workers have demonstrated that delocalized protons in hydrogen-bonded systems have several broad con-

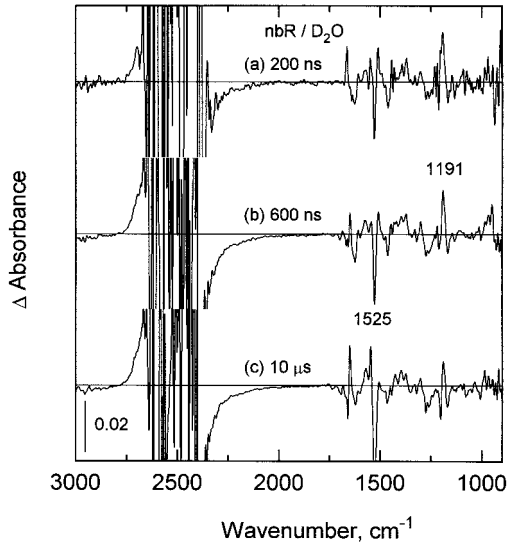

FIGURE 5 Time-resolved FTIR difference spectra in the bR photocycle in D_2O in the frequency range of 3000–1000 cm^{-1}, measured at room temperature, at delay times as follows: (*a*) 200 ns; (*b*) 600 ns; (*c*) 10 μs. The spectra show that the continua observed in H_2O at >2700 cm^{-1}, 2500–2150 cm^{-1}, and 2100–1800 cm^{-1} (Fig. 2) are not observed in D_2O. This strongly suggests that the continuum absorption in the 3000–1800-cm^{-1} band results in from the oscillating motion of protons (The strong noise-like signal between 2750 and 2200 cm^{-1} is due to the absorption of D_2O in this region).

tinuum bands in the mid-infrared region (Zundel and Brzezinski, 1992). In such a hydrogen-bonded network, a large proton polarizability results from the delocalization of proton into a hydrogen-bonded chain, which gives rise to an absorption continuum. These researchers showed that such continua are observed when the hydrogen-bonded dimer is homogeneous (H—A···H—A) or heterogeneous (H—A···H—B). It is also observed between hydrogen bonds involving cations (e.g., $—N^+$-H···C—R_2) and anions (e.g., ═C—O^-···H—O—R).

It should be mentioned that a polarizable hydrogen-bonded proton system has continua in more than one region with different intensities. Thus, during the photocycle of bR, as the polarizable hydrogen-bonded systems are changing, the intensity of the continua spectra for different intermediates changes in different regions by different amounts. Therefore, what we observe in each region at different times is the net change of the bleach due to the disappearance of the photolyzed bR and of the absorption due to the appearance of intermediates on the time scale examined. The observation of a net transient continuum absorption in a certain region of the spectrum signals the formation of one or more polarizable hydrogen-bonded systems that are more intense than those of the bleached one(s) in bR ground state.

The present results show a net absorption continuum in the 2100–1800-cm^{-1} region with two rise times of <80 and 190 ns and two decay components of 60 and 300 μs (see Figs. 3 and 4). Previous studies (Riesle et al., 1996; Rammelsberg et al., 1998; Wang and El-Sayed, 2000) showed a transient bleach (instead of absorption) in the frequency region of 1900–1800 cm^{-1} that is formed within hundreds of microseconds. In the present study, the decay time determined for the transient absorption in the 2100–1800-cm^{-1} region is in agreement with the previously reported rise times for the formation of the observed bleach band in the 1900–1800-cm^{-1} region (50–70 μs). However, there is an apparent difference in the assignment of spectral characteristics (absorption versus bleach). We believe the reason for this is the baseline correction that is related directly to the infrared bandpass filter used in the step-scan mode of FTIR. In the present study, we use a bandpass filter that covers the entire 3000–500-cm^{-1} range, which is much broader than most of the band filters used in the previous studies (Rammelsberg et al., 1998; Wang and El-Sayed, 2000) that cover only the 1900–900-cm^{-1} region. Therefore, a decay process of a small positive transient absorption signal at a certain frequency observed in the broad spectral region could be seen as a formation process of a small negative transient bleach signal at the cutoff frequency portion of a narrow bandpass filter.

The molecular origin of the polarizable hydrogen-bonded proton continua in bR

The net bleach continuum spectra in the 2500–2150-cm^{-1} region and above 2700 cm^{-1} appear upon the formation of K and decay in 300 μs. Thus, one or more polarizable hydrogen-bonded protons present in bR change upon retinal photoisomerization. This polarizable hydrogen-bonded system must be within the active site and very close to the retinal molecule. Thus, beside the observed bleach continuum, the formation of K is accompanied by the formation of one or more polarizable hydrogen-bonded systems, which gives the observed net absorption in the 2100–1800-cm^{-1} region. This continuum has two rise times of <80 and 190 ns and two decay times of 50–60 μs and 300 μs. Because the component that rises in <80 ns and decays in 300 μs has similar kinetics as that of the observed bleach continua, one is tempted to assign it to the polarizable hydrogen-bonded system resulting from the photoisomerization. The other component that rises in 190 ns and decays in 50–60 μs could thus be another polarizable hydrogen-bonded system that is involved in pumping the proton to the surface. This is because the L-to-M transition occurs in ~50–60 μs. It is also on the same time scale as the appearance of the pumped proton to the surface (Heberle and Dencher, 1992; Alexiev et al., 1995) and that for the deprotonation of Tyr185, as determined optically (Dupuis et al., 1985) and from FTIR difference spectroscopy (Rothschild et al., 1990a).

From the x-ray studies (Edman et al., 1999; Luecke et al., 1999b), one can propose two possible polarizable hydrogen-bonded systems in bR. The first one is between the PSB and

a water molecule (water 402) (N^+—H···OH_2). The second one is between Tyr185 and Asp212 (—Ph—O—H···$O^-{}_2C$—). They could form either two independent hydrogen-bonded systems or just one system. For example, the one system could involve the PSB, water 402, Asp85, Tyr185, Asp212, and water 401, as concluded from the recent x-ray structure of bR (Luecke et al., 1999a). In K, there is no doubt that this stable hydrogen-bonded structure is disturbed upon retinal photoisomerization. There are several independent studies whose results suggest a large change in the charge distribution takes place in the bR-K transition. Movement of a water molecule occurs (Edman et al., 1999) and Tyr185 seems to become partially deprotonated (Rothschild et al., 1990a), and a rapid charge separation is detected (Keszthelyi and Ormos, 1983; Trissl, 1990; Liu and Ebrey, 1988; Liu, 1990) that has a rise time of $<$30 ps (Groma et al., 1984). Thus, the changes in the nature of the polarizable hydrogen bonds upon K formation might be responsible for the appearance of the net absorption in the 2100–1800-cm^{-1} region and the observed net bleach in the region of 2500–2150 cm^{-1} and above 2700 cm^{-1}.

The FTIR difference spectrum between bR and trapped K (Rothschild et al., 1990a) showed that the degree of Tyr185 protonation changes, as monitored by the 1277- and 1272-cm^{-1} bands that are absent in the Asp212 mutant. This led them to conclude that a polarizable hydrogen bond exists between Tyr185 and Asp212 in bR, which leads to the shift of Tyr185 hydrogen toward Asp212 upon K formation. One might then conclude that this contributes to the net bleach and net absorption continua during the bR-to-K transformation. If indeed the two polarizable hydrogen-bonded systems (the PSB···H_2O(402) and Tyr185···Asp212) change during the formation of K, one can assign the fast component in the absorption continuum ($<$90 ns) to changes in the PSB···H_2O (402) system and the slow component (190 ns) to changes in the Tyr185···Asp212 system. This is because one might expect that the structure around the C═N^+H moiety of the PSB changes on the same time scale as the photoisomerization time scale (0.5 ps).

Optical spectroscopy has also shown that during the M formation, some tyrosine residues deprotonate on the same time scale as the deprotonation of PSB (Scherrer et al., 1981; Lemke and Oesterhelt, 1981; Lam et al., 1983; Dupuis and El-Sayed, 1985). This tyrosine residue has been shown later to be Tyr185 (Dunach et al., 1990). The fact that the absorption continuum in the 2100–1800-cm^{-1} region appears with a slow component of 190 ns and its short component disappears upon M formation strongly suggests our assignment that the polarizable hydrogen bond between Asp212 and Tyr185 makes a good contribution to it. Upon K formation a displacement of Tyr185 hydrogen of the hydroxyl group occurs in the Tyr185···Asp212 hydrogen-bonded system. In the L-to-M transition, this hydrogen is ionized completely. The recovery of the ground-state bleach in 300 μs cannot be due to a polarizable hydrogen-bonded proton involving the PSB or the tyrosinate because both of these recover on a much longer time scale (outside our limit). It must then involve water molecules that do not affect the absorption of the retinal or the tryosinate ion. Of course, it could also result from the formation of a new polarizable hydrogen-bonded proton system whose intensity compensates that of the bleach of the ground state in this frequency region.

The polarizable hydrogen-bonded chains and the proton pump mechanism

It has been found that the Schiff base proton is transferred to Asp85 but remains bound to it until the recovery of bR at the end of the photocycle (Siebert et al., 1982; Bousche et al., 1992; Souvignier and Gerwert, 1992). Another proton appears on the surface on the same time scale as the protonation of Asp85 (Heberle and Dencher, 1990, 1992; Scherrer et al., 1992; Heberle et al., 1993). Active research has been carried out in the past decade aimed at identifying the molecular origin of the proton being pumped to the surface and thus the mechanism of the proton pump process itself. The proton-releasing process has been proposed to involve Arg82 (Otto et al., 1990; Balashov et al., 1993, 1995; Govindjee et al., 1996), Glu204 (Misra et al., 1997; Kandori et al., 1997; Richter et al., 1996; Brown et al., 1995, 1996), Glu194 (Dioumaev et al., 1998), and Arg134 (Lu et al., 2000) residues. Earlier, other proposals suggested that an ionized internal water molecule could be the source of the surface protons (El-Sayed et al., 1995).

The transport of the proton to the surface via a chain of water molecules was proposed as early as 1981 (Nagle and Mille, 1981), long before any spectroscopic experimental evidence of the presence of internal water molecules was reported. The presence of internal water molecules in the active site of bR has been detected by using Raman spectroscopy (Hildebrandt and Stockburger, 1984; Deng et al., 1994; Althaus et al., 1995), by FTIR (Chang et al., 1991; Maeda et al., 1992; Fischer et al., 1994), by neutron diffraction (Papadopoulos et al., 1990), by nuclear magnetic resonance (NMR) (Lugtenburg et al., 1988), and recently by x-ray diffraction (Pebay-Peyroula et al., 1997; Luecke et al., 1999b).

Recently, a proton pump mechanism was proposed (Luecke et al., 1999a) from the observed changes in the x-ray diffraction upon M formation. In this model, the changes in the pKa of different residues resulting from changes in the water structure within the hydrophobic interior of the protein is proposed to lead to the final deprotonation of Glu204. There are, however, a number of facts for which this model does not account. 1) Time-resolved FTIR studies showed that Glu204 is not deprotonated in M. 2) Tyr185 is deprotonated in M but not in this model. 3) Both the PSB and Tyr185 deprotonate at the same time as the appearance of the proton on the surface. And 4) three of the seven internal

water molecules disappear upon the M formation (water 402, 406, and 403).

Because Glu204 is not deprotonated in M, there must be another source for the proton appearing on the surface in M. From the above observations, one concludes that the source of the proton that appears on the surface could either come from Tyr185 or from one of the disappearing water molecules. Tyr185 can give up its proton to initiate a rapid transport proton on the hydrogen-bonded chain made of water and other residues to reach the surface. It needs a trigger for its complete deprotonation process that should be turned on in about the same time as that for the proton transfer from the PSB to Asp85 via water 402. If as discussed above, there is a strongly coupled hydrogen-bonded network involving the two hydrogen-bonded polarizable protons (that of the PSB and that of Tyr185), then the trigger could simply be the motion of one or more water molecules. This could decrease the pKa of both the PSB and Tyr185 and/or decrease the pKb of the conjugated base of Asp85 and Asp212 acids. Theoretical calculation is needed to examine this possible mechanism.

It was previously suggested (El-Sayed, 1992), that the trigger could involve an interior cation, stabilized by a cluster of two to three water molecules and O^- of the carboxylate groups of the amino acid residues. In the L-M transition, a simultaneous exposure of the PSB and Tyr185 to the positive charge on this cation can take place (Dupuis et al., 1985). This greatly reduces the pKa values of both the PSB and Tyr185 as a result of the repulsion between the cation and the PSB and the attraction between the tyrosinate anion and the cation. This model offers a switch that ionizes the PSB proton and the Tyr185 proton on a comparable time scale. The PSB proton is transferred to Asp85 and the Tyr185 proton is transferred to the surface via a hydrogen-bonded water chain.

It was also proposed previously (El-Sayed et al., 1995) that Asp85 might be one of the ligands that stabilizes the metal cation (together with water 402 and other water molecules). As it gets neutralized, one of the water molecules (e.g., water 402) ionizes, giving rise to one proton and one OH^-. The OH^- group substitutes for Asp85 as a ligand to stabilize the metal cation. The resulting proton could thus be transferred to the surface via the hydrogen-bonded chains present in the system. In this model, the metal cation switch might even release two protons, one from Tyr185 and another one from a water molecule, only one of them will be transferred to the surface via the hydrogen-bonded network shown in the x-ray studies (Edman et al., 1999; Luecke et al., 1999a,b).

As attractive as it is, the above model requires a metal cation to be bound within the reaction center that is ligated to water molecules, and few amino acid residues. This metal cation complex can communicate effectively with the surface through the hydrogen-bonded network. There are many references in the literature supporting the presence of one or two specific interior cation-binding sites (Chang et al., 1985; Dupuis et al., 1985; Chronister et al., 1986; Ariki and Lanyi, 1986; Corcoran et al., 1987; Dunach et al., 1987; Jonas et al., 1990; Mitra and Stroud, 1990; Zhang et al., 1992, 1993; Yang and El-Sayed, 1995; Stuart et al., 1995; Yoo et al., 1995; El-Sayed et al., 1995; Tan et al., 1996; Birge et al., 1996) as well as those supporting the presence of only surface binding sites for all metal cations (Szundi and Stoeckenius, 1987, 1988, 1989; Fu et al., 1997; Tuzi et al., 1999; Varo et al., 1999). The fact that the recent x-ray structures of bR confirm the presence of a number of internal bound water molecules (Edman et al., 1999; Luecke et al., 1999a) makes the proposal of having an interior metal cation not out of the question. Furthermore, the presence of a hydrogen-bonded network connecting the extracellular surface to the reaction center is expected to keep the reaction center with its PSB and Asp85 in rapid equilibrium with the surface potential. This might eliminate the most serious results against the internal binding sites that are based on the observations correlating the surface potential to the protonation state of Asp85 and the color change of the retinal. Previous theoretical calculations (Tan et al., 1996; Pardo et al., 1998) have already shown the possibility of having a metal cation within the reaction center. With the recent three-dimensional atomic structure data of bR, now known exactly, a more accurate ab initio calculation can be used to find out whether or not a cation can bind within the reaction center of bR.

Possible conclusions

Combining previous spectroscopic and x-ray studies and the present results one reaches the following possible conclusions. 1) More than one hydrogen-bonded chain exists in bR that changes upon retinal photoisomerization. 2) One of them involves the PSB-H_2O(402)-Asp85 and is responsible for the transfer of the proton from the PSB to Asp85 through the water molecule during M formation. 3) Another chain involves the Tyr185 and Asp212. 4) These two chains could also be one large chain involving PSB-H_2O(402), Asp85, Tyr185, Asp212, and H_2O(401) and other water molecules (e.g., 406). 5) The previously observed similar deprotonation rate of the PSB and Tyr185 could be explained by the presence of one trigger. 6) This trigger could be the photoisomerization process followed by H_2O rearrangements of the water molecules around the PSB and Try185 (and Asp212) that leads to changes in their pKa values. 7) This trigger could also be the approach and interaction of an interior metal cation with both the PSB and Tyr185. 8) The source of the pumped surface proton could thus be Tyr185 and/or an ionizable H_2O molecule ligated to the metal cation.

We thank the Chemical Sciences, Geosciences and Biosciences Division, Office of Basic Energy Sciences, Office of Sciences, U.S. Department of

Energy (under grant DE-FG02–97ER14799) for financial support. We also thank Mr. Colin Heyes for proof reading the manuscript.

REFERENCES

Alexiev, U., R. Mollaaghababa, P. Scherrer, H. G. Khorana, and M. P. Heyn. 1995. Rapid long-range proton diffusion along the surface of the purple membrane and delayed proton transfer into the bulk. *Proc. Natl. Acad. Sci. U S.A.* 92:372–376.

Althaus, T., W. Eisfeld, R. Lohrmann, and M. Stockburger. 1995. Application of Raman spectroscopy to retinal proteins. *Israel J. Chem.* 35: 227–251.

Ariki, M., and J. K. Lanyi. 1986. Characterization of metal ion-binding sites in bacteriorhodopsin. *J. Biol. Chem.* 261:8167–8174.

Atkinson, G. H., L. Ujj, and Y. Zhou. 2000. Vibrational spectrum of the J-625 intermediate in the room temperature bacteriorhodopsin photocycle. *J. Phys. Chem. A.* 104:4130–4139.

Balashov, S. P., R. Govindjee, E. S. Imasheva, S. Misra, T. G. Ebrey, Y. Feng, R. K. Crouch, and D. R. Menick. 1995. The two pKa's of aspartate-85 and control of thermal isomerization and proton release in the arginine-82 to lysine mutant of bacteriorhodopsin. *Biochemistry.* 34:8820–8834.

Balashov, S. P., R. Govindjee, M. Kono, E. Imasheva, E. Lukashev, T. G. Ebrey, R. K. Crouch, D. R. Menick, and Y. Feng. 1993. Effect of the arginine-82 to alanine mutation in bacteriorhodopsin on dark adaptation, proton release, and the photochemical cycle. *Biochemistry.* 32: 10331–10343.

Birge, R. R. 1981. Photophysics of light transduction in rhodopsin and bacteriorhodopsin. *Annu. Rev. Biophys. Bioeng.* 10:315–354.

Birge, R. R., D. S. K. Govender, K. C. Izgi, and E. H. L. Tan. 1996. Role of calcium in the proton pump of bacteriorhodopsin: microwave evidence for a cation-gated mechanism. *J. Phys. Chem.* 100:9990–10004.

Bousche, O., S. Sonar, M. P. Krebs, H. G. Khorana, and K. J. Rothschild. 1992. Time-resolved Fourier transform infrared spectroscopy of the bacteriorhodopsin mutant Tyr-185→Phe: Asp-96 reprotonates during O formation; Asp-85 and Asp-212 deprotonate during O decay. *Photochem. Photobiol.* 56:1085–1095.

Braiman, M. S., T. Mogi, T. Marti, L. J. Stern, H. G. Khorana, and K. J. Rothschild. 1988. Vibrational spectroscopy of bacteriorhodopsin mutants: light-driven proton transport involves protonation changes of aspartic acid residues 85, 96, and 212. *Biochemistry.* 27:8516–8520.

Brown, L. S., R. Needleman, and J. K. Lanyi. 1996. Interaction of proton and chloride transfer pathways in recombinant bacteriorhodopsin with chloride transport activity: implications for the chloride translocation mechanism. *Biochemistry.* 35:16048–16054.

Brown, L. S., J. Sasaki, H. Kandori, A. Maeda, R. Needleman, and J. K. Lanyi. 1995. Glutamic acid 204 is the terminal proton release group at the extracellular surface of bacteriorhodopsin. *J. Biol. Chem.* 270: 27122–27126.

Chang, C. H., J. G. Chen, R. Govindjee, and T. Ebrey. 1985. Cation binding by bacteriorhodopsin. *Proc. Natl. Acad. Sci. U.S.A.* 82: 396–400.

Chang, C. W., N. Sekiya, and K. Yoshihara. 1991. Oxygen-hydrogen stretching vibration in Fourier transform difference infrared spectra of bacteriorhodopsin. *FEBS Lett.* 287:157–159.

Chen, W. G., and M. S. Braiman. 1991. Kinetic analysis of time-resolved infrared difference spectra of the L and M intermediates of bacteriorhodopsin. *Photochem. Photobiol.* 54:905–910.

Chronister, E. L., T. C. Corcoran, L. Song, and M. A. El-Sayed. 1986. On the molecular mechanisms of the Schiff base deprotonation during the bacteriorhodopsin photocycle. *Proc. Natl. Acad. Sci. U.S.A.* 83: 8580–8584.

Corcoran, T. C., K. Z. Ismail, and M. A. El-Sayed. 1987. Evidence for the involvement of more than one metal cation in the Schiff base deprotonation process during the photocycle of bacteriorhodopsin. *Proc. Natl. Acad. Sci. U.S.A.* 84:4094–4098.

Dencher, N. A., G. Papadopoulos, D. Dresselhaus, and G. Bueldt. 1990. Light- and dark-adapted bacteriorhodopsin, a time-resolved neutron diffraction study. *Biochim. Biophys. Acta.* 1026:51–56.

Deng, H., L. Huang, R. Callender, and T. Ebrey. 1994. Evidence for a bound water molecule next to the retinal Schiff base in bacteriorhodopsin and rhodopsin: a resonance Raman study of the Schiff base hydrogen/deuterium exchange. *Biophys. J.* 66:1129–1136.

Dioumaev, A. K., H.-T. Richter, L. S. Brown, M. Tanio, S. Tuzi, H. Saito, Y. Kimura, R. Needleman, and J. K. Lanyi. 1998. Existence of a proton transfer chain in bacteriorhodopsin: participation of Glu-194 in the release of protons to the extracellular surface. *Biochemistry.* 37: 2496–2506.

Dunach, M., S. Berkowitz, T. Marti, Y. W. He, S. Subramaniam, H. G. Khorana, and K. J. Rothschild. 1990. Ultraviolet-visible transient spectroscopy of bacteriorhodopsin mutants: evidence for two forms of tyrosine-185 in phenylalanine. *J. Biol. Chem.* 265:16978–16984.

Dunach, M., M. Seigneuret, J. L. Rigaud, and E. Padros. 1987. Characterization of the cation binding sites of the purple membrane: electron spin resonance and flash photolysis studies. *Biochemistry.* 26:1179–1186.

Dupuis, P., T. C. Corcoran, and M. A. El-Sayed. 1985. Importance of bound divalent cations to the tyrosine deprotonation during the photocycle of bacteriorhodopsin. *Proc. Natl. Acad. Sci. U.S.A.* 82:3662–3664.

Dupuis, P., and M. A. El-Sayed. 1985. Effect of salt on the tyrosine and protonated Schiff base deprotonation kinetics in bacteriorhodopsin. *Can. J. Chem.* 63:1699–1704.

Earnest, T. N., P. Roepe, M. S. Braiman, J. Gillespie, and K. J. Rothschild. 1986. Orientation of the bacteriorhodopsin chromophore probed by polarized Fourier transform infrared difference spectroscopy. *Biochemistry.* 25:7793–7798.

Ebrey, T. G. 1993. Light Energy Transduction in Bacteriorhodopsin. CRC Press, New York.

Edman, K., P. Nollert, A. Royant, H. Belrhali, E. Pebay-Peyroula, J. Hajdu, R. Neutze, and E. Landau. 1999. High-resolution x-ray structure of an early intermediate in the bacteriorhodopsin photocycle. *Nature.* 401: 822–826.

El-Sayed, M. A. 1992. On the molecular mechanisms of the solar to electric energy conversion by the other photosynthetic system in nature, bacteriorhodopsin. *Accounts of Chemical Research.* 25:279–286.

El-Sayed, M. A., D. Yang, S.-K. Yoo, and N. Zhang. 1995. The effect of different metal cation binding on the proton pumping in bacteriorhodopsin. *Israel J. Chem.* 35:465–474.

Essen, L. O., R. Siegert, w. D. Lehmann, and D. Oesterhelt. 1998. Lipid patches in membrane protein oligomers: crystal structure of the bacteriorhodopsin-lipid complex. *Proc. Natl. Acad. Sci. U.S.A.* 95: 11673–11678.

Fischer, W. B., S. Sonar, T. Marti, H. G. Khorana, and K. J. Rothschild. 1994. Detection of a water molecule in the active site of bacteriorhodopsin: hydrogen bonding changes during the primary photoreaction. *Biochemistry.* 33:12757–12762.

Fu, X., S. Bressler, M. Ottolenghi, T. Eliash, N. Friedman, and M. Sheves. 1997. Titration kinetics of Asp-85 in bacteriorhodopsin: exclusion of the retinal pocket as the color-controlling cation binding site. *FEBS Lett.* 416:167–170.

Govindjee, R., S. Misra, S. P. Balashov, T. G. Ebrey, R. K. Crouch, and D. R. Menick. 1996. Arginine-82 regulates the pKa of the group responsible for the light-driven proton release in bacteriorhodopsin. *Biophys. J.* 71:1011–1023.

Groma, G. I., G. Szabo, and G. Varo. 1984. Direct measurement of picosecond charge separation in bacteriorhodopsin. *Nature.* 308: 557–558.

Heberle, J., and N. A. Dencher. 1990. Bacteriorhodopsin in ice: accelerated proton transfer. *FEBS Lett.* 277:277–280.

Heberle, J., and N. A. Dencher. 1992. Surface-bound optical probes monitor proton translocation and surface potential changes during the bacteriorhodopsin photocycle. *Proc. Natl. Acad. Sci. U.S.A.* 89:5996–6000.

Heberle, J., D. Oesterhelt, and N. A. Dencher. 1993. Decoupling of photo- and proton cycle in the Asp85→Glu mutant of bacteriorhodopsin. *EMBO J.* 12:3721–3727.

Henderson, R. 1979. The structure of bacteriorhodopsin and its relevance to other membrane proteins. *Soc. Gen. Physiol. Ser.* 33:3–15.

Henderson, R., J. M. Baldwin, T. A. Ceska, F. Zemlin, E. Beckmann, and K. H. Downing. 1990. Model for the structure of bacteriorhodopsin based on high-resolution electron cryo-microscopy. *J. Mol. Biol.* 213: 899–929.

Hildebrandt, P., and M. Stockburger. 1984. Role of water in bacteriorhodopsin's chromophore: resonance Raman study. *Biochemistry.* 23: 5539–5548.

Jonas, R., Y. Koutalos, and T. G. Ebrey. 1990. Purple membrane: surface charge density and the multiple effect of pH and cations. *Photochem. Photobiol.* 52:1163–1177.

Kandori, H., N. Kinoshita, Y. Shichida, and A. Maeda. 1998. Protein structural changes in bacteriorhodopsin upon photoisomerization as revealed by polarized FTIR spectroscopy. *J. Phys. Chem. B.* 102: 7899–7905.

Kandori, H., Y. Yamazaki, M. Hatanaka, R. Needleman, L. S. Brown, H.-T. Richter, J. K. Lanyi, and A. Maeda. 1997. Time-resolved Fourier transform infrared study of structural changes in the last steps of the photocycles of Glu-204 and Leu-93 mutants of bacteriorhodopsin. *Biochemistry.* 36:5134–5141.

Keszthelyi, L., and P. Ormos. 1983. Displacement current on purple membrane fragments oriented in a suspension. *Biophys. Chem.* 18: 397–405.

Koch, M. H. J., N. A. Dencher, D. Oesterhelt, H. J. Ploehn, G. Rapp, and G. Bueldt. 1991. Time-resolved x-ray diffraction study of structural changes associated with the photocycle of bacteriorhodopsin. *EMBO J.* 10:521–526.

Lam, E., S. Seltzer, T. Katsura, and L. Packer. 1983. Light-dependent nitration of bacteriorhodopsin. *Arch. Biochem. Biophys.* 227:321–328.

Lanyi, J. K. 1993. Proton translocation mechanism and energetics in the light-driven pump bacteriorhodopsin. *Biochim. Biophys. Acta.* 1183: 241–261.

Lemke, H. D., and D. Oesterhelt. 1981. The role of tyrosine residues in the function of bacteriorhodopsin: specific nitration of tyrosine 26. *Eur. J. Biochem.* 115:595–604.

Liu, S. Y. 1990. Light-induced currents from oriented purple membrane. I. Correlation of the microsecond component (B2) with the L-M photocycle transition. *Biophys. J.* 57:943–950.

Liu, S. Y., and T. G. Ebrey. 1988. Photocurrent measurements of the purple membrane oriented in a polyacrylamide gel. *Biophys. J.* 54:321–329.

Lu, M., S. P. Balashov, T. G. Ebrey, N. Chen, Y. Chen, D. R. Menick, and R. K. Crouch. 2000. Evidence for the rate of the final step in the bacteriorhodopsin photocycle being controlled by the proton release group: R134H mutant. *Biochemistry.* 39:2325–2331.

Luecke, H., H.-T. Richter, and J. K. Lanyi. 1998. Proton transfer pathways in bacteriorhodopsin at 2.3 angstrom resolution. *Science.* 280: 1934–1937.

Luecke, H., B. Schobert, H.-T. Richter, J.-P. Cartailler, and J. K. Lanyi. 1999a. Structural changes in bacteriorhodopsin during ion transport at 2 angstrom resolution. *Science.* 286:255–260.

Luecke, H., B. Schobert, H.-T. Richter, J.-P. Cartailler, and J. K. Lanyi. 1999b. Structure of bacteriorhodopsin at 1.55 A resolution. *J. Mol. Biol.* 291:899–911.

Lugtenburg, J., R. A. Mathies, R. G. Griffin, and J. Herzfeld. 1988. Structure and function of rhodopsins from solid state NMR and resonance Raman spectroscopy of isotopic retinal derivatives. *Trends Biochem. Sci.* 13:388–393.

Maeda, A., J. Sasaki, Y. Shichida, and T. Yoshizawa. 1992. Water structural changes in the bacteriorhodopsin photocycle: analysis by Fourier transform infrared spectroscopy. *Biochemistry.* 31:462–467.

Mathies, R. A., C. H. B. Cruz, W. T. Pollard, and C. V. Shank. 1988. Direct observation of the femtosecond excited-state *cis-trans* isomerization in bacteriorhodopsin. *Science.* 240:777–779.

Mathies, R. A., S. W. Lin, J. B. Ames, and W. T. Pollard. 1991. From femtoseconds to biology: mechanism of bacteriorhodopsin's light-driven proton pump. *Annu. Rev. Biophys. Biophys. Chem.* 20:491–518.

Merz, H., and G. Zundel. 1986. Thermodynamics of proton transfer in carboxylic acid-retinal Schiff base hydrogen bonds with large proton polarizability. *Biochem. Biophys. Res. Commun.* 138:819–825.

Misra, S., R. Govindjee, T. G. Ebrey, N. Chen, J. X. Ma, and R. K. Crouch. 1997. Proton uptake and release are rate-limiting steps in the photocycle of the bacteriorhodopsin mutant E204Q. *Biochemistry.* 36:4875–4883.

Mitra, A. K., and R. M. Stroud. 1990. High sensitivity electron diffraction analysis: a study of divalent cation binding to purple membrane. *Biophys. J.* 57:301–311.

Mueller, K. H., H. J. Butt, E. Bamberg, K. Fendler, B. Hess, F. Siebert, and M. Engelhard. 1991. The reaction cycle of bacteriorhodopsin: an analysis using visible absorption, photocurrent and infrared techniques. *Eur. Biophys. J.* 19:241–251.

Nagle, J. F., and M. Mille. 1981. Molecular models of proton pumps. *J. Chem. Phys.* 74:1367–1372.

Nilsson, A., P. Rath, J. Olejnik, M. Coleman, and K. J. Rothschild. 1995. Protein conformational changes during the bacteriorhodopsin photocycle: a Fourier transform infrared/resonance Raman study of the alkaline form of the mutant Asp-85 .fwdarw. Asn. *J. Biol. Chem.* 270:29746–29751.

Nuss, M. C., W. Zinth, W. Kaiser, E. Koelling, and D. Oesterhelt. 1985. Femtosecond spectroscopy of the first events of the photochemical cycle in bacteriorhodopsin. *Chem. Phys. Lett.* 117:1–7.

Oka, T., H. Kamikubo, F. Tokunaga, J. K. Lanyi, R. Needleman, and M. Kataoka. 1999. Conformational change of helix G in the bacteriorhodopsin photocycle: investigation with heavy atom labeling and x-ray diffraction. *Biophys. J.* 76:1018–1023.

Olejnik, J., B. Brzezinski, and G. Zundel. 1992. A proton pathway with large proton polarizability and the proton pumping mechanism in bacteriorhodopsin: Fourier transform difference spectra of photoproducts of bacteriorhodopsin and of its pentademethyl analog. *J. Mol. Struct.* 271:157–173.

Otto, H., T. Marti, M. Holz, T. Mogi, L. J. Stern, F. Engel, H. G. Khorana, and M. P. Heyn. 1990. Substitution of amino acids Asp-85, Asp-212, and Arg-82 in bacteriorhodopsin affects the proton release phase of the pump and the pK of the Schiff base. *Proc. Natl. Acad. Sci. U.S.A.* 87:1018–1022.

Papadopoulos, G., N. A. Dencher, G. Zaccai, and G. Bualdt. 1990. Water molecules and exchangeable hydrogen ions at the active center of bacteriorhodopsin localized by neutron diffraction: elements of the proton pathway? *J. Mol. Biol.* 214:15–19.

Pardo, L., F. Sepulcre, J. Cladera, M. Dunach, A. Labarta, J. Tejada, and E. Padros. 1998. Experimental and theoretical characterization of the high-affinity cation-binding site of the purple membrane. *Biophys. J.* 75:777–784.

Pebay-Peyroula, E., G. Rummel, J. P. Rosenbusch, and E. M. Landau. 1997. X-ray structure of bacteriorhodopsin at 2.5 angstroms from microcrystals grown in lipidic cubic phases. *Science.* 277:1676–1681.

Petrich, J. W., J. Breton, J. L. Martin, and A. Antonetti. 1987. Femtosecond absorption spectroscopy of light-adapted and dark-adapted bacteriorhodopsin. *Chem. Phys. Lett.* 137:369–375.

Rammelsberg, R., G. Huhn, M. Luebben, and K. Gerwert. 1998. Bacteriorhodopsin's intramolecular proton-release pathway consists of a hydrogen-bonded network. *Biochemistry.* 37:5001–5009.

Richter, H.-T., L. S. Brown, R. Needleman, and J. K. Lanyi. 1996. A linkage of the pKa's of asp-85 and glu-204 forms part of the reprotonation switch of bacteriorhodopsin. *Biochemistry.* 35:4054–4062.

Riesle, J., D. Oesterhelt, N. A. Dencher, and J. Heberle. 1996. D38 is an essential part of the proton translocation pathway in bacteriorhodopsin. *Biochemistry.* 35:6635–6643.

Rothschild, K. J. 1992. FTIR difference spectroscopy of bacteriorhodopsin: toward a molecular model. *J. Bioenerg. Biomembr.* 24:147–167.

Rothschild, K. J., M. S. Braiman, Y. W. He, T. Marti, and H. G. Khorana. 1990a. Vibrational spectroscopy of bacteriorhodopsin mutants: evidence for the interaction of aspartic acid 212 with tyrosine 185 and possible role in the proton pump mechanism. *J. Biol. Chem.* 265:16985–16991.

Rothschild, K. J., Y. W. He, T. Mogi, T. Marti, L. J. Stern, and H. G. Khorana. 1990b. Vibrational spectroscopy of bacteriorhodopsin

mutants: evidence for the interaction of proline-186 with the retinylidene chromophore. *Biochemistry.* 29:5954–5960.

Sasaki, J., A. Maeda, C. Kato, and H. Hamaguchi. 1993. Time-resolved infrared spectral analysis of the KL-to-L conversion in the photocycle of bacteriorhodopsin. *Biochemistry.* 32:867–871.

Scherrer, P., U. Alexiev, H. Otto, M. P. Heyn, T. Marti, and G. H. Khorana. 1992. Proton movement and surface charge in bacteriorhodopsin detected by selectively attached pH-indicators. *Colloq. INSERM.* 221: 205–211.

Scherrer, P., L. Packer, and S. Seltzer. 1981. Effect of iodination of the purple membrane on the photocycle of bacteriorhodopsin. *Arch. Biochem. Biophys.* 212:589–601.

Siebert, F., W. Maentele, and W. Kreutz. 1982. Evidence for the protonation of two internal carboxylic groups during the photocycle of bacteriorhodopsin: investigation by kinetic infrared spectroscopy. *FEBS Lett.* 141:82–87.

Smith, S. O., I. Hornung, R. Van der Steen, J. A. Pardoen, M. S. Braiman, J. Lugtenburg, and R. A. Mathies. 1986. Are C_{14}-C_{15} single bond isomerizations of the retinal chromophore involved in the proton-pumping mechanism of bacteriorhodopsin ? *Proc. Natl. Acad. Sci. U.S.A.* 83:967–971.

Souvignier, G., and K. Gerwert. 1992. Proton uptake mechanism of bacteriorhodopsin as determined by time-resolved stroboscopic-FTIR-spectroscopy. *Biophys. J.* 63:1393–1405.

Stoeckenius, W., and R. H. Lozier. 1974. Light energy conversion in Halobacterium-halobium. *J. Supramol. Struct.* 2:769–74.

Stuart, J. A., B. W. Vought, C.-F. Zhang, and R. R. Birge. 1995. The active site of bacteriorhodopsin: two-photon spectroscopic evidence for a positively charged chromophore binding site mediated by calcium. *Biospectroscopy.* 1:9–28.

Szundi, I., and W. Stoeckenius. 1987. Effect of lipid surface charges on the purple-to-blue transition of bacteriorhodopsin. *Proc. Natl. Acad. Sci. U.S.A.* 84:3681–3684.

Szundi, I., and W. Stoeckenius. 1988. Purple-to-blue transition of bacteriorhodopsin in a neutral lipid environment. *Biophys. J.* 54:227–232.

Szundi, I., and W. Stoeckenius. 1989. Surface pH controls purple-to-blue transition of bacteriorhodopsin: a theoretical model of purple membrane surface. *Biophys. J.* 56:369–383.

Tan, E. H. L., D. S. K. Govender, and R. R. Birge. 1996. Large organic cations can replace Mg^{2+} and Ca^{2+} ions in bacteriorhodopsin and maintain proton pumping ability. *J. Am. Chem. Soc.* 118:2752–2723.

Trissl, H. W. 1990. Photoelectric measurements of purple membranes. *Photochem. Photobiol.* 51:793–818.

Tuzi, S., S. Yamaguchi, M. Tanio, H. Konishi, S. Inoue, A. Naito, R. Needleman, J. K. Lanyi, and H. Saito. 1999. Location of a cation-binding site in the loop between helices F and G of bacteriorhodopsin as studied by ^{13}C NMR. *Biophys. J.* 76:1523–1531.

Van den Berg, R., D. J. Jang, H. C. Bitting, and M. A. El-Sayed. 1990. Subpicosecond resonance Raman spectra of the early intermediates in the photocycle of bacteriorhodopsin. *Biophys. J.* 58:135–141.

Varo, G., L. S. Brown, R. Needleman, and J. K. Lanyi. 1999. Binding of calcium ions to bacteriorhodopsin. *Biophys. J.* 76:3219–3226.

Wang, J.-P., and M. A. El-Sayed. 2000. Proton polarizability of hydrogen-bonded network and its role in proton transfer in bacteriorhodopsin. *J. Phys. Chem. A.* 104:4333–4337.

Wolfgang, H., K. Munsok, H. Frei, and R. A. Mathies. 1996. Protein dynamics in the bacteriorhodopsin photocycle: a nanosecond step-scan FTIR investigation of the KL to L transition. *J. Phys. Chem.* 100: 16026–16033.

Yang, D., and M. A. El-Sayed. 1995. The Ca^{2+} binding to deionized monomerized and to retinal removed bacteriorhodopsin. *Biophys. J.* 69:2056–2059.

Yoo, S.-K., E. S. Awad, and M. A. El-Sayed. 1995. Comparison between the binding of Ca^{2+} and Mg^{2+} to the two high-affinity sites of bacteriorhodopsin. *J. Phys. Chem.* 99:11600–11604.

Zhang, Y. N., M. A. El-Sayed, M. L. Bonet, J. K. Lanyi, M. Chang, B. Ni, and R. Needleman. 1993. Effects of genetic replacements of charged and hydrogen-bonding residues in the retinal pocket on calcium binding to deionized bacteriorhodopsin. *Proc. Natl. Acad. Sci. U.S.A.* 90: 1445–1449.

Zhang, Y. N., L. L. Sweetman, E. S. Awad, and M. A. El-Sayed. 1992. Nature of the individual calcium binding sites in Ca^{2+}-regenerated bacteriorhodopsin. *Biophys. J.* 61:1201–1206.

Zscherp, C., R. Schlesinger, J. Tittor, D. Oesterhelt, and J. Heberle. 1999. In situ determination of transient pKa changes of internal amino acids of bacteriorhodopsin by using time-resolved attenuated total reflection Fourier-transform infrared spectroscopy. *Proc. Natl. Acad. Sci. U.S.A.* 96:5498–5503.

Zundel, G. 1994. Hydrogen-bonded chains with large proton polarizability as charge conductors in proteins bacteriorhodopsin and the F0 subunit of *E. coli*. *J. Mol. Struct.* 322:33–42.

Zundel, G., and B. Brzezinski. 1992. Proton polarizability of hydrogen-bonded systems due to collective proton motion: with a remark on the proton pathways in bacteriorhodopsin. *Adv. Sci. Inst. Ser. B Physics.* 291:153–166.

Zundel, G., and H. Merz. 1984. On the role of hydrogen bonds and hydrogen-bonded systems with large proton polarizability for mechanisms of proton activation and conduction in bacteriorhodopsin. *Prog. Clin. Biol. Res.* 164:153–164.